Supplementary Materials for

An ambient-stable and stretchable ionic skin with multimodal sensation

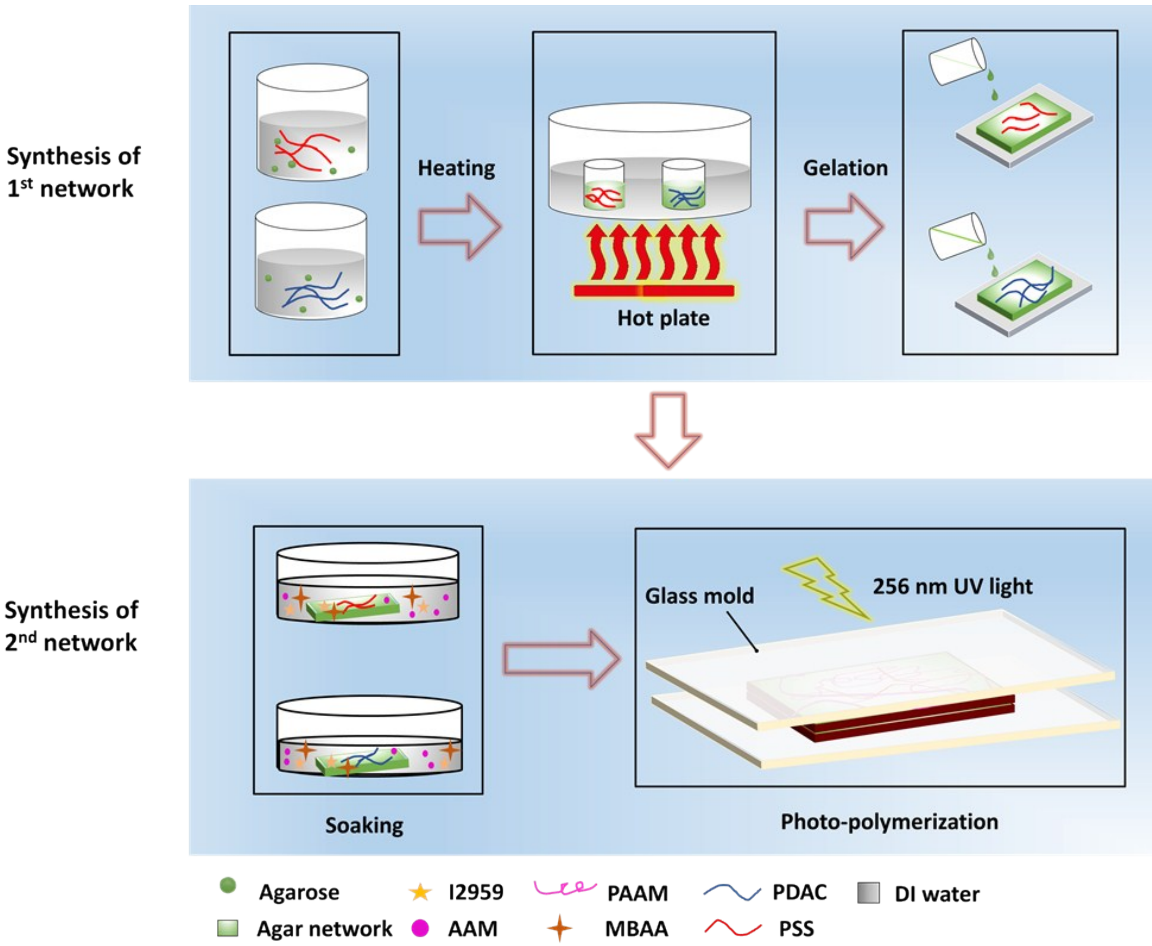

Fig. S1. Two-step synthesis of AIskin.

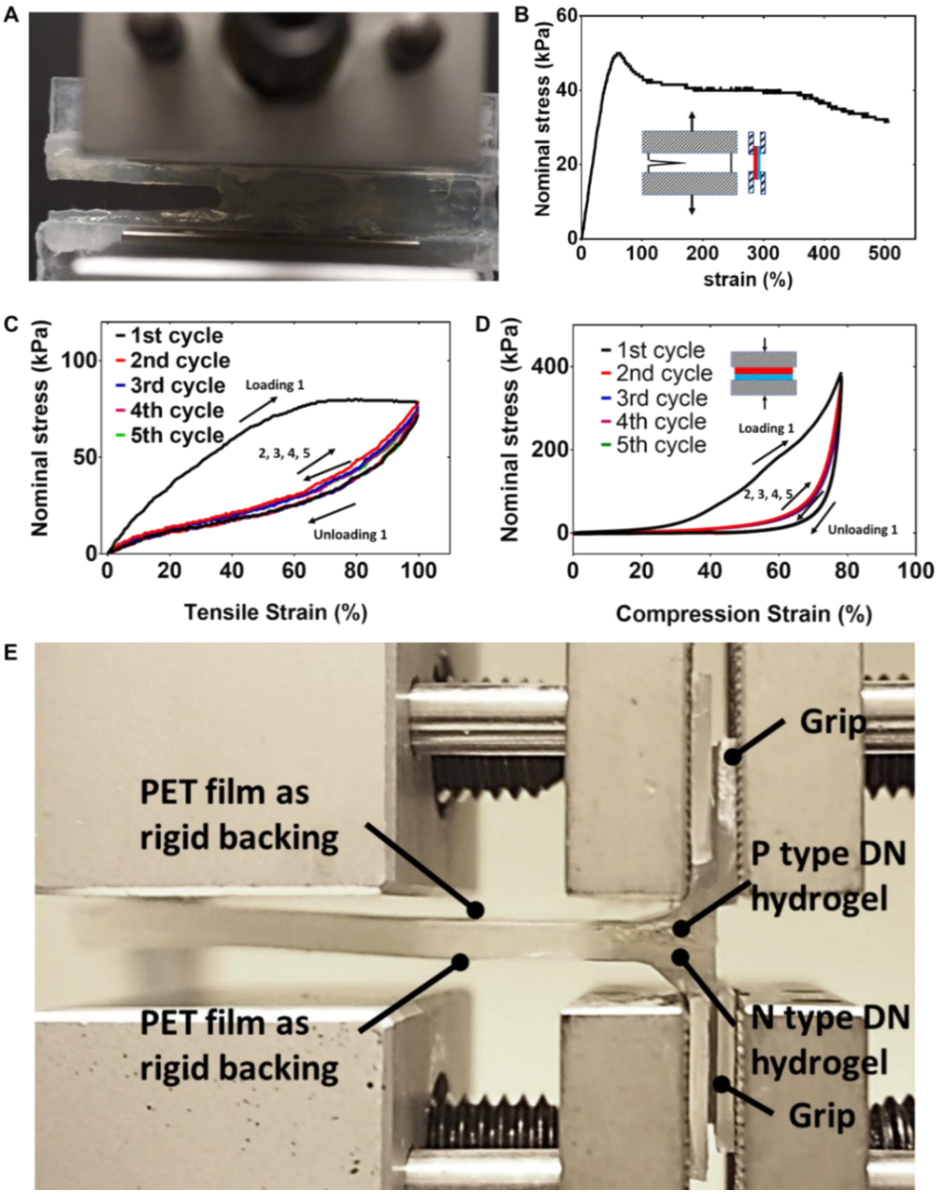

Fig. S2. Mechanical performance of the AIskin. (**A**) Pure-shear test for measuring the toughness of an AIskin. A piece of hydrogel with a notch was stretched until the crack propagates. (**B**) Stress-strain curve of the AIskin. (**C**) Five successive tensile loading-unloading cycles of an AIskin at the maximum strain of 100%. **(D)** Five successive compression loading-unloading cycles of an AIskin at a maximum strain of 80%. **(E)** Peeling adhesion test. Digital photo showing the AIskin under 180-degree peeling test, in which two surfaces of hydrogel were glued to a PET film to eliminate energy dissipation in regions away from the crack tip. Two open ends of hydrogel with grip were stretched with a universal testing machine.

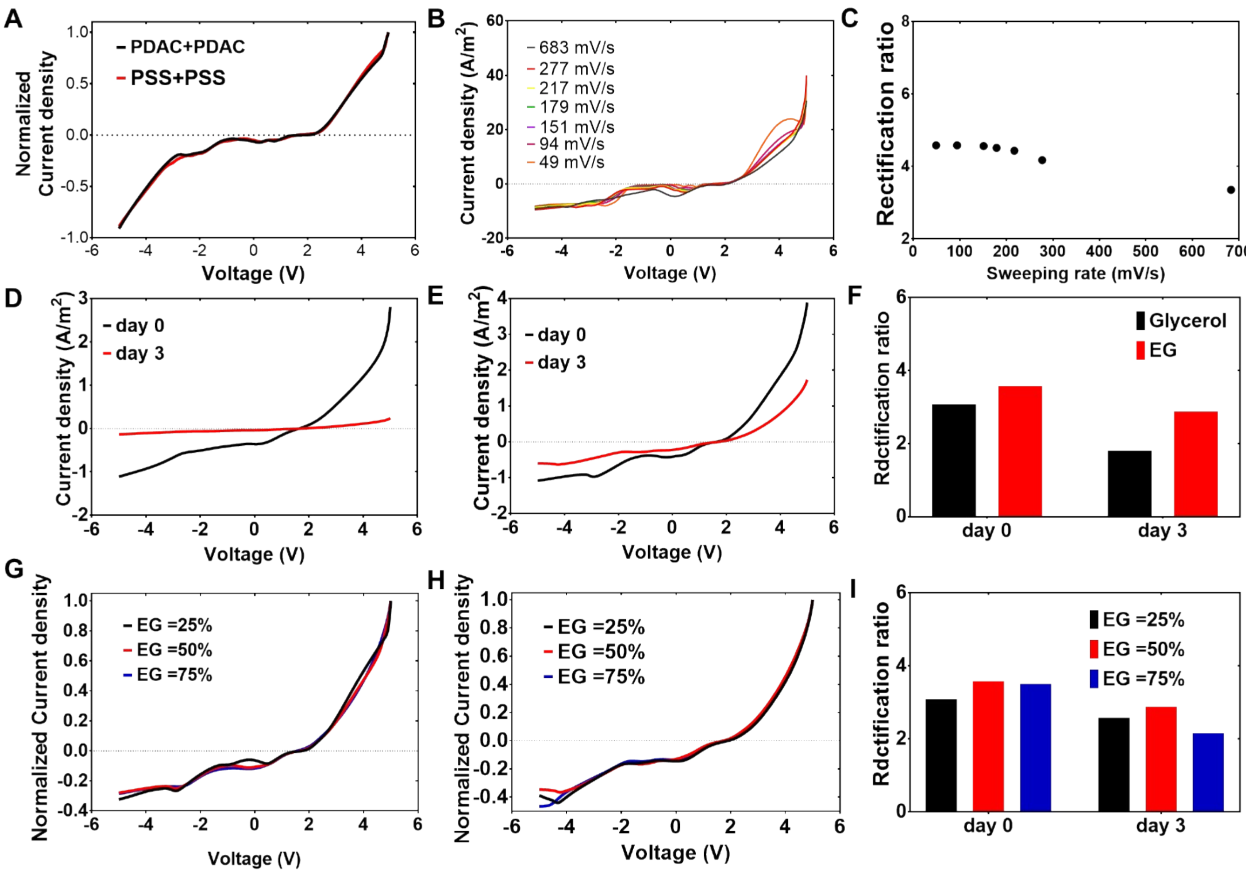

Fig. S3. Rectification effect of an AIskin at different conditions. (A) Voltage-current curves for the hydrogel skin with the same charge density. (**B**) Voltage-current curves and (**C**) Rectification ratio of an AIskin at different sweeping rates. **(D)** Voltage-current curves for an ambient stable AIskin with 50 v/v % glycerol on day 0 and day 3. (**E**) Voltage-current curves for an ambient stable AIskin with 50 v/v % EG on day 0 and day 3. (**F**) Rectification ratio is compared between two hygroscopic materials on day 0 and day 3. (**G**) Voltage-current curves for ambient stable AIskin with different EG concentrations on day 0. (**H**) Voltage-current curves for ambient stable AIskin with different EG concentrations on day 3. (**I**) Rectification ratio is compared between ambient stable AIskin with different concentrations of EG on day 0 and day 3.

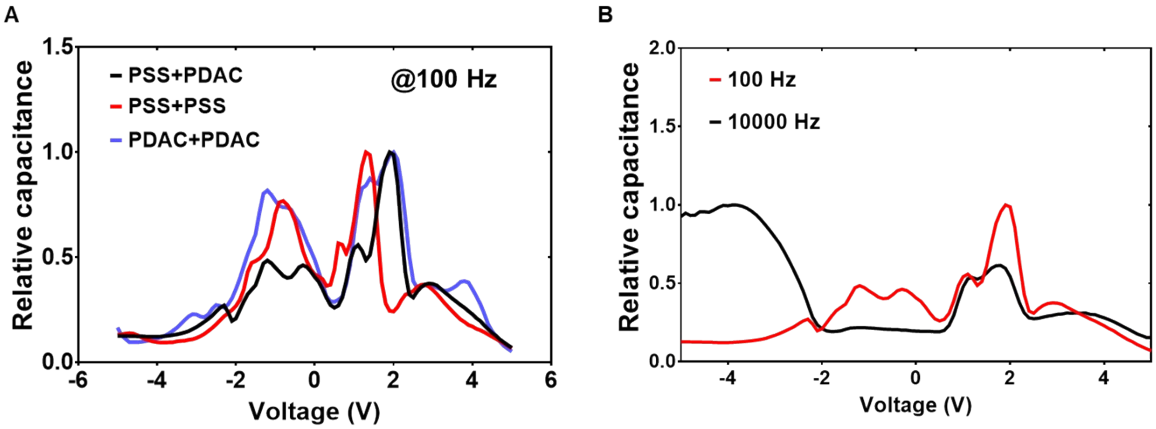

Fig. S4. Capacitance-voltage (C-V) response of different types of biolayer hydrogels. (**A**) Comparison between AIskin, bilayer PSS hydrogel and bilayer PDAC hydrogel when the scan frequency is 100 Hz. (**B**) Comparison of the C-V responses of the same AIskin under low (100 Hz) and high (10000 Hz) scan frequencies. All the devices were washed for 4 h before tests.

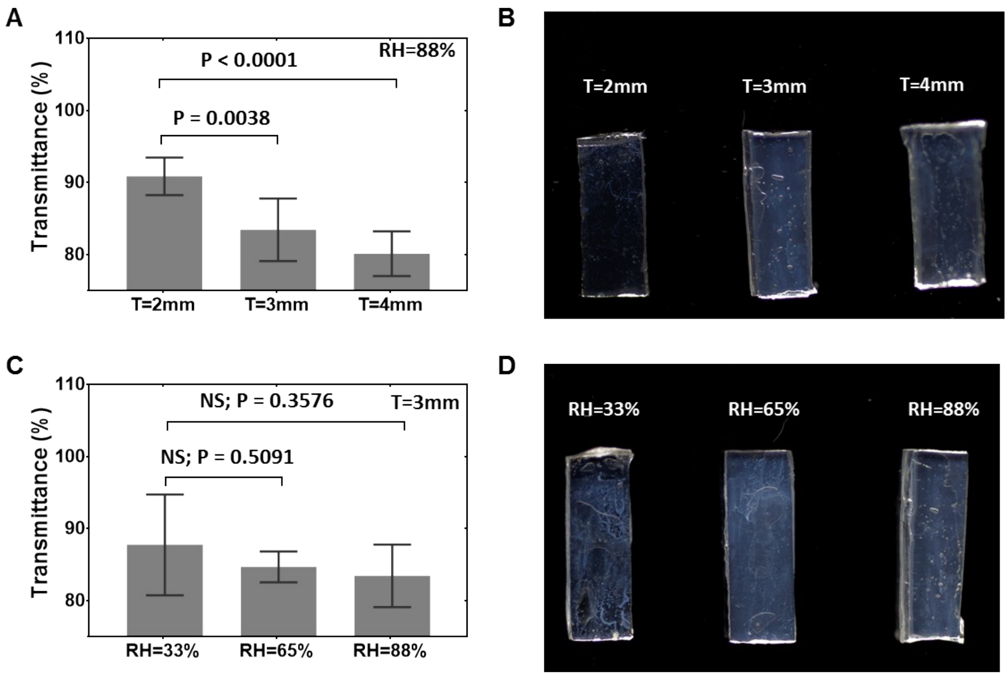

Fig. S5. Transmittance of EG-laden AIskin at the wavelength of 700 nm with different experimental conditions. (**A**) RH = 88%, and thickness varies from 2 mm to 4 mm. (**B**) Optical photographs showing the transparency of samples with different thicknesses. (**C**) Thickness = 3mm, RH varies from 33% to 88%. (**D**) Optical photographs showing the transparency of samples under different RH values. All the samples were stored in humidity chambers for at least 3 days before transmittance measurement.

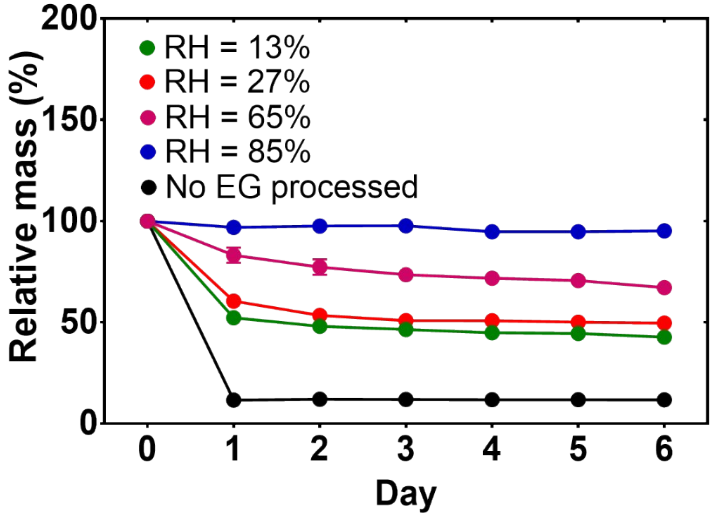

Fig. S6. Measurement of water loss as a function of RHs. The mass of AIskin is normalized with its initial mass (N = 3).

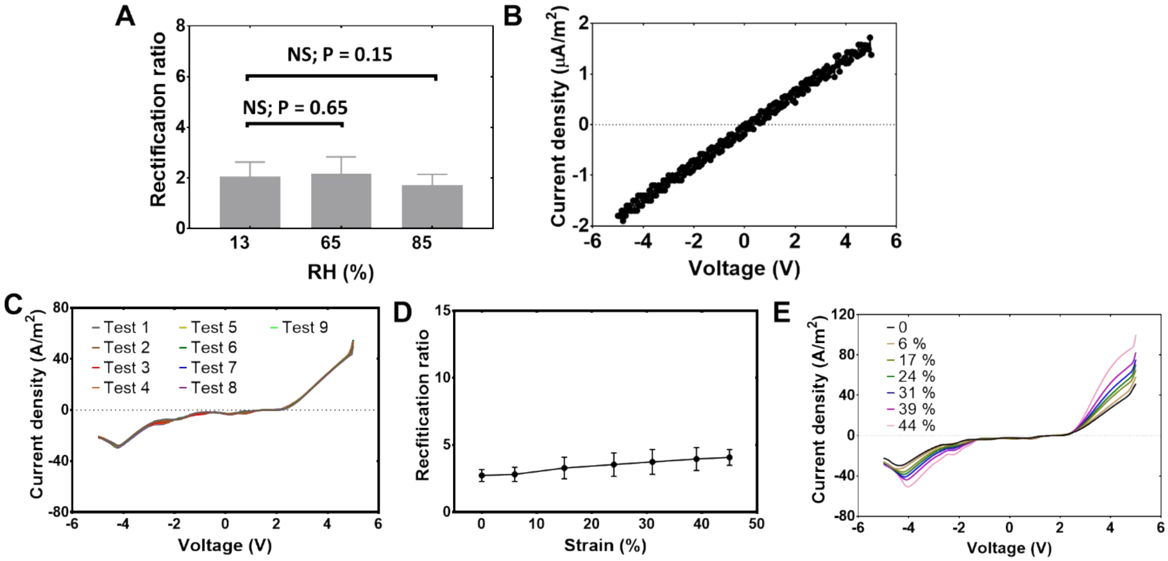

Fig. S7. Rectifying effect of AIskin at different RHs and strains. (**A**) Rectification ratios of AIskin at different RHs after storage for 3 days (N=9). NS: not significant. (**B**) Voltage-current curves of an AIskin without EG after 3-day storage at RH 13%. (**C**) Repeated I-V testing results of an AIskin under the laboratory environment (21 °C and relative humidity of 60~65%). Between each measurement, the device was electrically shorted for 60 s. (**D**) Rectification ratio of an AIskin under different strains (N=3). (**E**) Voltage-current curves of an AIskin under different strains. The AI skin used in **Fig. S7.** C-D was washed for 2 h.

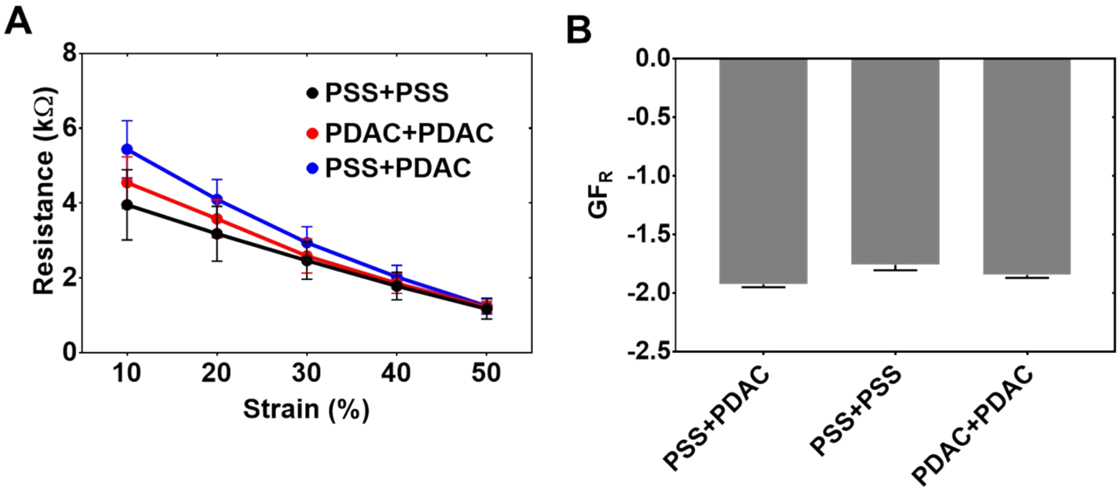

Fig. S8. Resistance-strain relations of the AIskin, PSS hydrogel and PDAC hydrogel. (**A**) Resistance-strain curves of the AIskin, PSS and PDAC DN hydrogels (N=3-4). The compressive strains vary from 10% to 50%. (**B**) Resistive gauge factors (GF_R) among the AIskin, bilayer PSS and bilayer PDAC hydrogels.

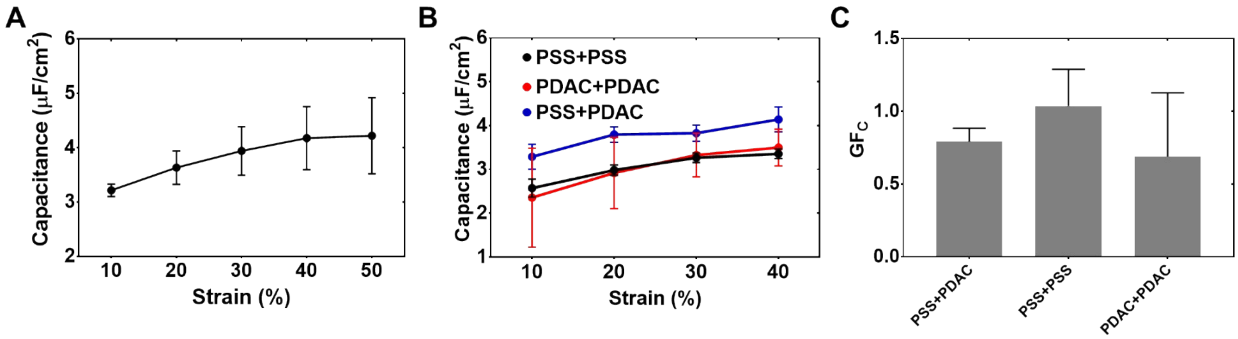

Fig. S9. Capacitance-strain relations of the AIskin, PSS hydrogel, and PDAC hydrogel. (**A**) Capacitance-strain curves of the ambient stable AIskin at the RH of 65% (N=3). The compressive strains vary from 10% to 50%. The capacitance is normalized by the area of electrode-hydrogel contact. (**B**) Capacitance-strain curves of the AIskin, PSS and PDAC DN hydrogel (N=3-4). The compressive strains vary from 10% to 40%. (**C**) Capacitive gauge factors (GF_C) among the AIskin, bilayer PSS and bilayer PDAC hydrogels.

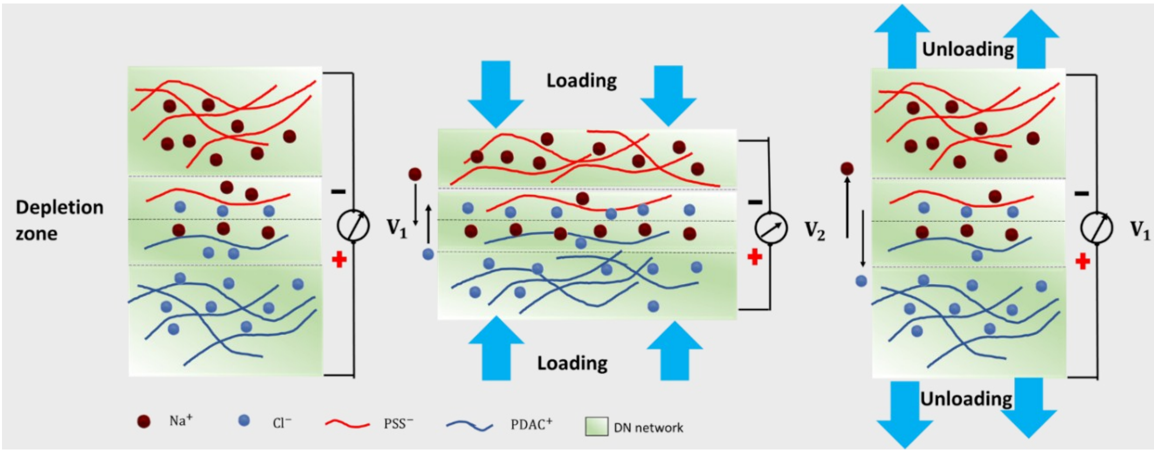

Fig. S10. Schematic mechanism of OCV change with applied deformation on an AIskin.

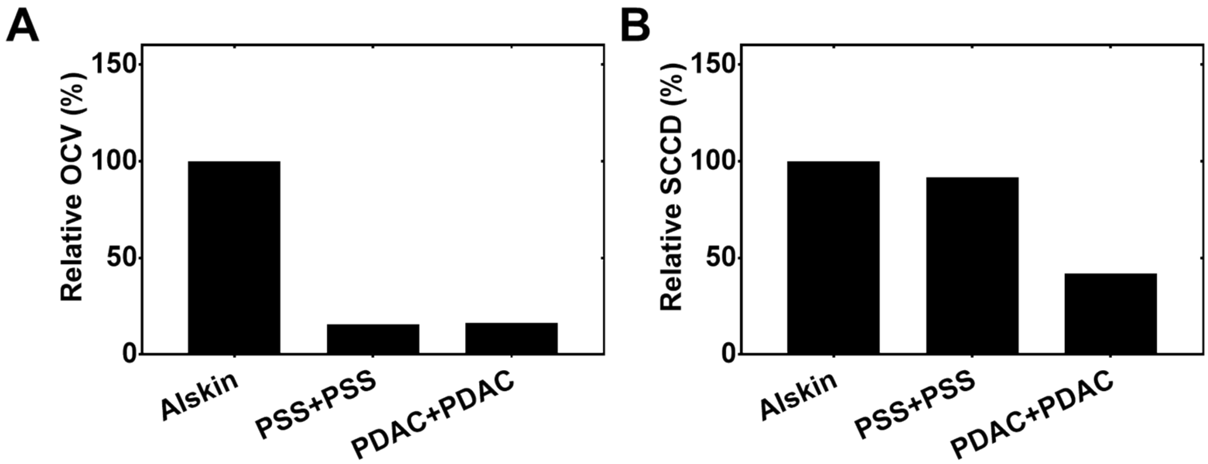

Fig. S11. Self-generating capability of the AIskin, PSS hydrogel, and PDAC hydrogel. (**A**) Relative OCV of the AIskin, bilayer PSS and bilayer PDAC hydrogels. **(B)** Relative SCCD of the AIskin, bilayer PSS and bilayer PDAC hydrogels. The compressive strain is 50% and the strain speed is 10% s^{-1} for all three devices.

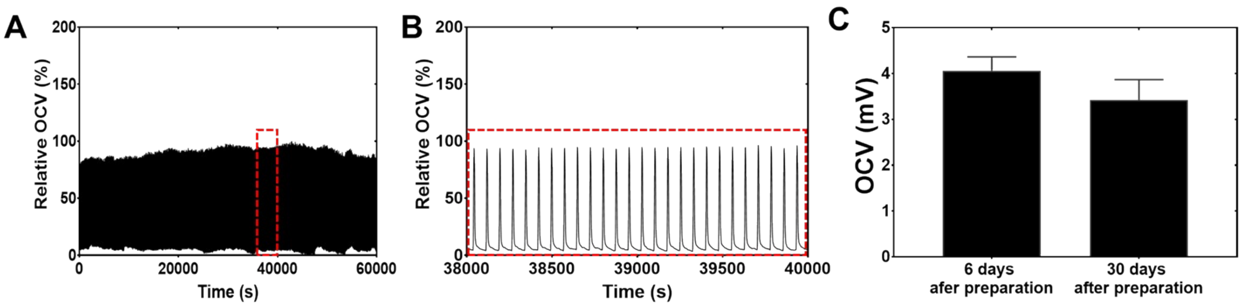

Fig. S12. Durability and stability of the AIskin for the use of strain sensor. OCV is measured as a representative signal in this study. (**A**) Durability of OCV signals after ~1000 cycles of repeated loading-unloading steps at the RH of 13%. The strain is 50%. (**B**). Zoom-in plot of **Fig. S12.** A. (**C**) Stability of OCV signals over one-month storage at the RH of 65% (N=3).

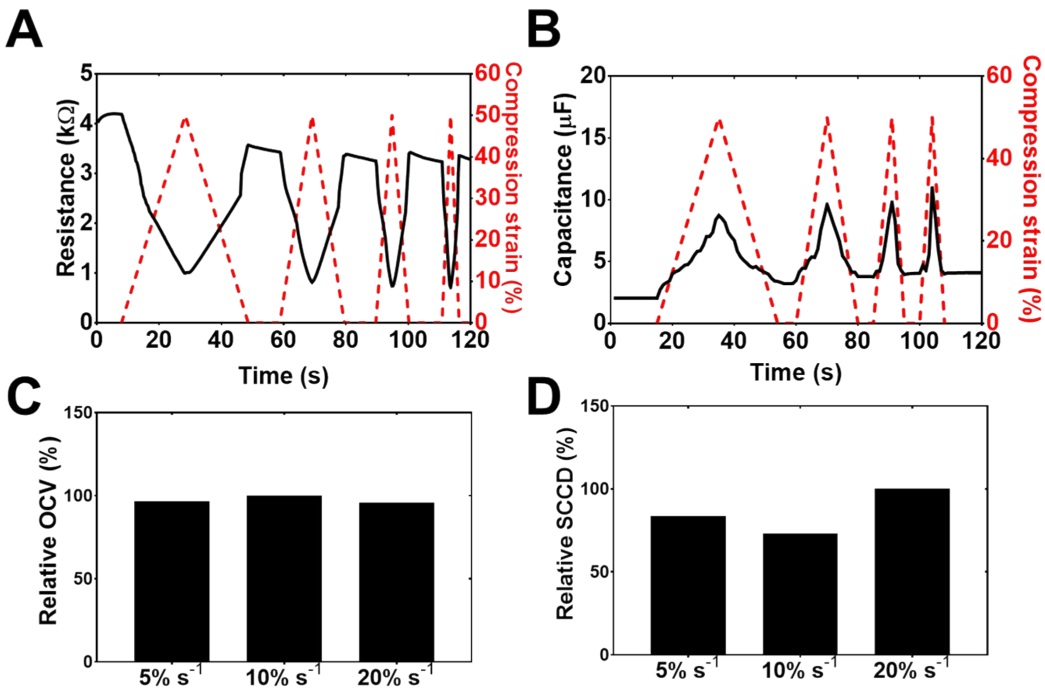

Fig. S13. Sensing robustness of AIskin under different strain rates. (**A**) Resistance curve at specific strain rates (2.5% s^{-1},5% s^{-1}, 10% s^{-1} and 20% s^{-1}). (**B**) Capacitance curve at specific strain rates (2.5% s^{-1},5% s^{-1}, 10% s^{-1} and 20% s^{-1}). (**C**) Relative OCV at specific strain rates (5% s^{-1}, 10% s^{-1} and 20% s^{-1}). (**D**) Relative SCCD at specific strain rates (5% s^{-1}, 10% s^{-1} and 20% s^{-1}). The compressive strain is set at 50%.

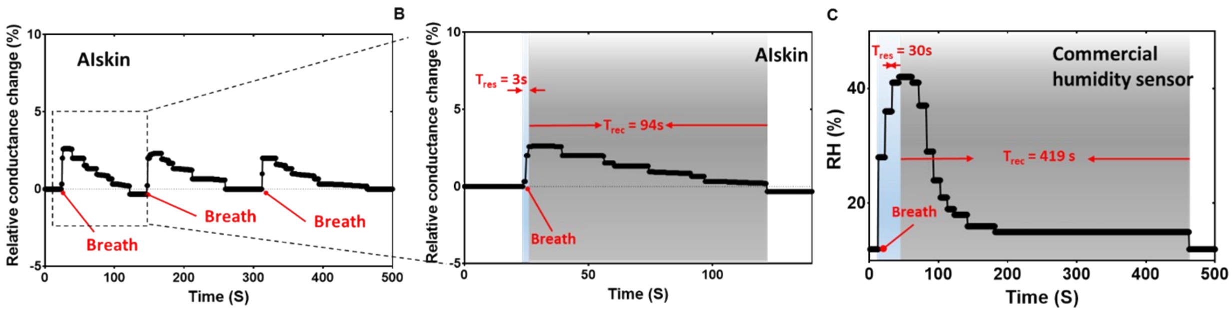

Fig. S14. Comparison of the response and recovery time between our AIskin and a commercial hygrometer (B0778C8C9L, AMIR). (**A**) Relative conductance changes of an EG-laden AIskin with a thickness of 300 µm with repeated human breath applied. (**B**) Zoomed-in view of one response cycle (response time: 3s, and recovery time: 94s) in **Fig. S14**A. (**C**) The response (response time: 30s, and recovery time: 419s) of the commercial hygrometer to one human breath.

Movie S1. Pure shear test to show the stretchability and toughness of the AIskin.

Movie S2. AIskin sandwiched between VHB films mounted on a finger joint to show high transparency and stretchability.

Movie S3. Human-machine interaction by using a four-button artificial skin with self-generated signals to control the movement of a greedy snake.